

# A Mathematical Model of the Ionospheric Electric Field which Closes the Global Electric Circuit

Valery V. Denisenko<sup>1,2</sup>,  
Michael J. Rycroft<sup>3,4</sup>, R. Giles Harrison<sup>5,6</sup>

<sup>1</sup> Institute of Computational Modelling RAS SB, Krasnoyarsk, Russia

<sup>2</sup> Siberian Federal University, Krasnoyarsk, Russia

<sup>3</sup> CAESAR Consultancy, Cambridge, UK

<sup>4</sup> Centre for Space, Atmospheric and Oceanic Science, Department of Electronic and Electrical Engineering, University of Bath, UK

<sup>5</sup> Department of Meteorology, University of Reading, UK

<sup>6</sup> Department of Electronic and Electrical Engineering, University of Bath, UK

A model for the distribution of the ionospheric electric potential which drives the currents which close the global electric circuit is constructed. Only the internal electric fields and currents generated by thunderstorms are studied. The atmospheric conductivity profiles with altitude are empirically determined, and the topography of the Earth's surface is taken into account. A two-dimensional approximation of the ionospheric conductor is based on large conductivities along the geomagnetic field; the Pedersen and Hall conductivity distributions are calculated using the empirical models IRI, MSIS and IGRF.

The maximum calculated voltage difference in the ionosphere under typical conditions for July, under low solar activity, at 19 : 00 UT, is about 85 V. The ionospheric electric fields are found to be an order of magnitude smaller than those of the well-known model of Hays and Roble, 1979.

# 1 The Electric Conductivity Equation

The basic equations for the steady state electric field  $\mathbf{E}$  and current density  $\mathbf{j}$

$$\text{curl } \mathbf{E} = 0, \quad \text{div } \mathbf{j} = Q, \quad \mathbf{j} = \hat{\sigma} \mathbf{E}, \quad (1)$$

$\hat{\sigma}$  - the conductivity tensor,  $\mathbf{j}_{ext}$  - external current density,

$$Q = -\text{div } \mathbf{j}_{ext}$$

Electric potential  $V$ ,  $\mathbf{E} = -\text{grad } V$ .

Electric conductivity equation

$$-\text{div} (\hat{\sigma} \text{grad } V) = Q. \quad (2)$$

Spherical geomagnetic coordinates  $r, \theta_m, \varphi_m$ , geomagnetic latitude  $\lambda_m = \pi/2 - \theta_m$ , height above mean sea level  $h$ .

# 2 Separation of Ionospheric and Atmospheric Conductors

The Earth's ground is an ideal conductor

$$V|_{h=h_g(\theta, \varphi)} = -V_0, \quad (3)$$

the value of the constant  $V_0$  will be defined later.

Our model of the topography (Denisenko, Yakubailik, 2015).

We define the boundaries separating the ionosphere:

Atmosphere below  $h_I = 90$  km

Magnetosphere above  $h_M = 500$  km, nonzero conductivity across  $\mathbf{B}$  only in plasma sheet and cusps.

The whole magnetic field line in the ionosphere and magnetosphere is an equipotential object - 2-D model.

Domain decomposition.

### 3 Atmospheric Conductor

$$V|_{h=h_I} = 0. \quad (4)$$

Dirichlet boundary value problem (2-4) for the atmosphere that is simulated as a conductor between two ideal conductors. Unique solution when the constant  $V_0$  is given.

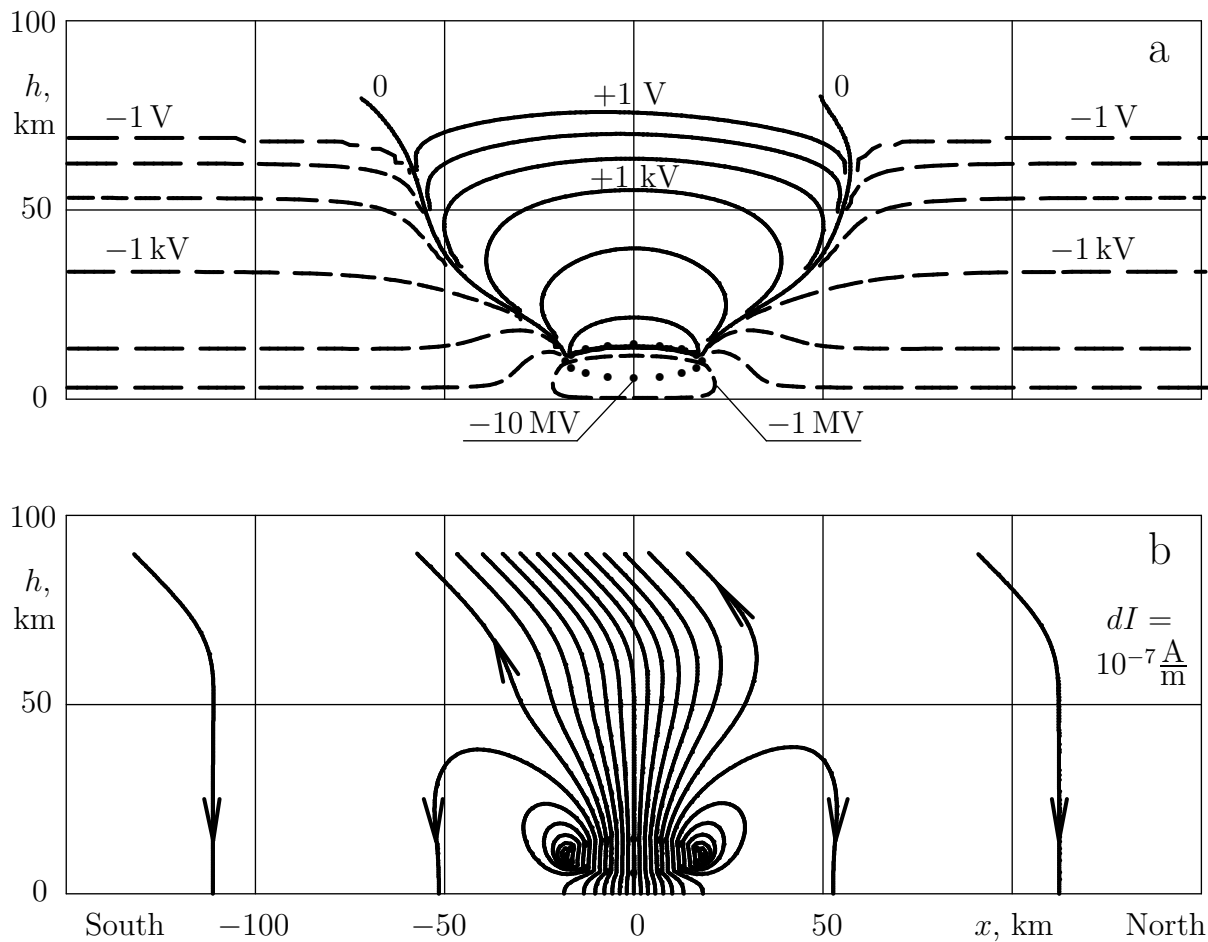


Рис. 1: The equipotentials – a, and the current lines for the total current – b in the neighborhood of a thunderstorm cloud. Dots show elliptical cross-sections of the cloud.

Obtained solutions around thunderstorm clouds (Fig. 1 and similar for an equatorial cloud) permit to project thunderstorms to the ionosphere.

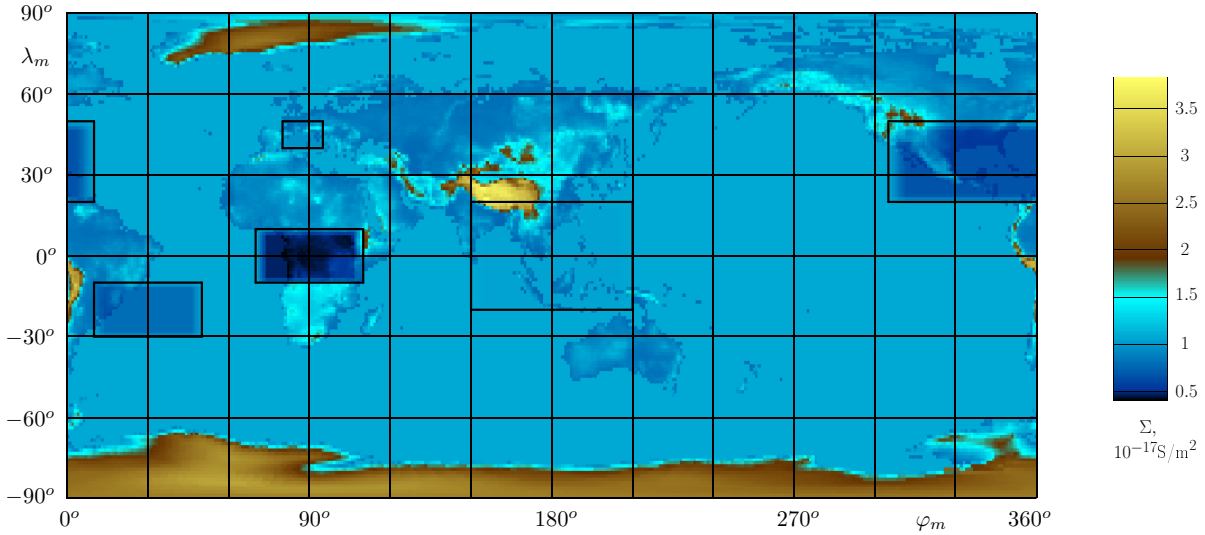


FIG. 2: The global distribution of the vertical conductance of the atmosphere  $\Sigma(\lambda_m, \varphi_m)$  in units of  $10^{-17}\text{S}/\text{m}^2$ . The rectangles show the regions with electric current to the ionosphere from thunderstorm clouds (Hays and Roble, 1979).

Because of the large horizontal scale we use the flat 1-D model instead of the 3-D equation

$$-\frac{d}{dh} \left( \sigma(h) \frac{d}{dh} V(h) \right) = 0, \quad V|_{h=h_0} = 0, \quad V|_{h=h_g(\theta, \varphi)} = -V_0. \quad (5)$$

The value  $V_0$  is taken to balance the total fair weather and thunderstorm currents.

Height distributions of the conductivity  $\sigma(h)$  similar to the empirical model (Rycroft, Odzimek, 2010):

fair weather vertical electric field strength  $E_0 = 130\text{V}/\text{m}$  near ground produces current density  $j_0 = 2\text{pA}/\text{m}^2$ ;

the potential difference between the ground and the ionosphere  $V_0 = 250\text{kV}$ .

The conductance of the atmospheric vertical column with

$1 \text{ m}^2$  cross-section between ground and ionosphere

$$\Sigma(\theta, \varphi) = 1 / \int_{h_g(\theta, \varphi)}^{h_0} \frac{dh}{\sigma(h)}. \quad (6)$$

## 4 Conductivity in the Earth's Ionosphere

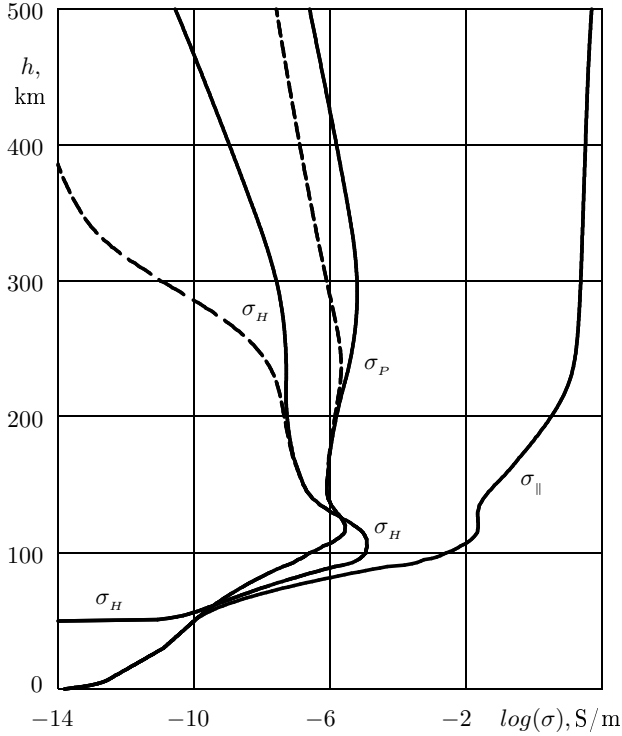


Рис. 3: Profiles of the components of the electric conductivity tensor for a mid-latitude night-time ionosphere. The effective Pedersen and Hall conductivity averaged during an acceleration period of 3 hours are presented by the dashed lines.

We use parallel and normal to the direction of magnetic induction  $\mathbf{B}$  components of vectors which are marked with symbols  $\parallel$  and  $\perp$ . Ohm's law (1) in a gyrotropic medium

$$\mathbf{j}_{\parallel} = \sigma_{\parallel} \mathbf{E}_{\parallel}, \quad \mathbf{j}_{\perp} = \sigma_P \mathbf{E}_{\perp} - \sigma_H [\mathbf{E}_{\perp} \times \mathbf{B}] / B, \quad (7)$$

Hall ( $\sigma_H$ ), Pedersen ( $\sigma_P$ ), field-aligned ( $\sigma_{\parallel}$ ) conductivities.

We have created the model (Denisenko, et al., 2008) to calculate the components  $\sigma_P$ ,  $\sigma_H$ ,  $\sigma_{\parallel}$  of the conductivity tensor  $\hat{\sigma}$ , that is based on the empirical models IRI, MSISE, IGRF.

2-D model, Pedersen and Hall conductances  $\Sigma_P, \Sigma_H$ :

$$\mathbf{J}_{\perp} = \begin{pmatrix} \Sigma_P & -\Sigma_H \\ \Sigma_H & \Sigma_P \end{pmatrix} \mathbf{E}_{\perp}, \quad (8)$$

$$\Sigma_P = \int \sigma_P dl, \quad \Sigma_H = \int \sigma_H dl. \quad (9)$$

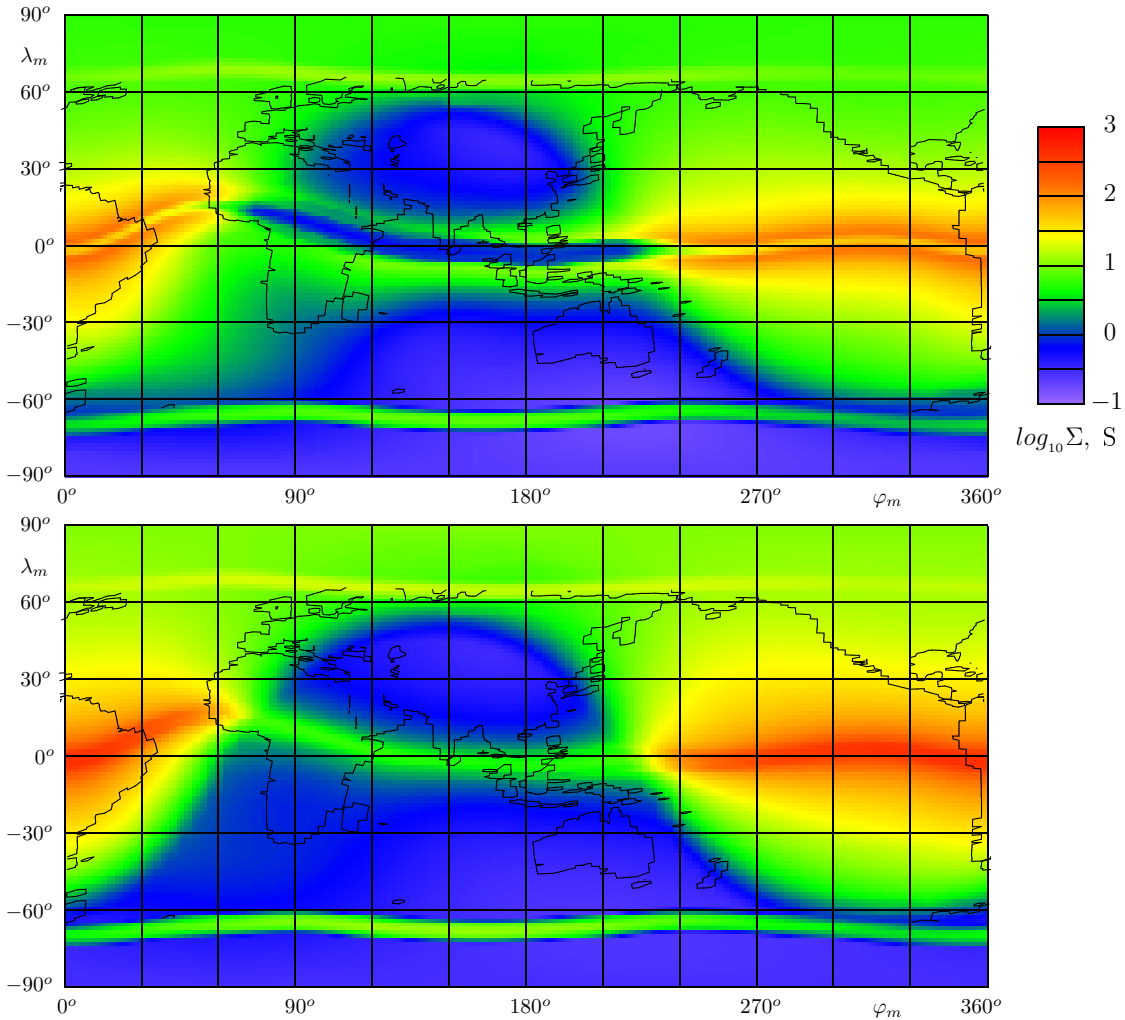


Рис. 4: Distribution of the integral Pedersen conductance  $\Sigma_P$  (top panel) and Hall conductance  $\Sigma_H$  (bottom panel). The points with  $\lambda_m, \varphi_m$  geomagnetic coordinates at 120 km height in the ionosphere identify halves of magnetic field lines. Maps are calculated under typical conditions for July under high solar activity at the considered point in time, 19:00 UT.

## 5 Boundary Value Problems

The charge conservation law in some plane with Cartesian coordinates  $x, y$  that presents all magnetic field

$$-\frac{\partial}{\partial x} \left( \Sigma_{xx} \frac{\partial V}{\partial x} + \Sigma_{xy} \frac{\partial V}{\partial y} \right) - \frac{\partial}{\partial y} \left( \Sigma_{yx} \frac{\partial V}{\partial x} + \Sigma_{yy} \frac{\partial V}{\partial y} \right) = Q_{ext}, \quad (10)$$

$Q_{ext}$  - the density of current from the atmosphere, transformed to the new coordinates  $x, y$ . For dipolar geomagnetic field  $\Sigma_{xx} = \Sigma_{yy} = \Sigma_P$ ,  $\Sigma_{xy} = \Sigma_{yx} = \Sigma_H$ . The partial differential equation (10) is an equation of elliptical type.

The auroral zones are equivalent to almost ideal conductors because they are connected in parallel with good (ideal) magnetospheric conductors:  $V = 0$  in the auroral zones. This condition cuts the ionosphere into three parts which are the Northern and Southern polar caps and the main part that contains middle- and low latitudes.

$$V|_{\Gamma_N} = 0, \quad V|_{\Gamma_S} = 0, \quad (11)$$

$$V|_{\Gamma_{aur}} = 0, \quad (12)$$

the boundaries of the Northern and Southern polar caps are  $\Gamma_N$  and  $\Gamma_S$ .

For the main part of the ionosphere the auroral and equatorial boundaries  $\Gamma_{aur}$ ,  $\Gamma_{eq}$ .  $\Gamma_{eq}$  corresponds to the last magnetic field lines which are regarded as ionospheric ones. As a consequence of the charge conservation law

$$J_\nu|_{\Gamma_{eq}} = -J_{eq}^0. \quad (13)$$

Our numerical method for the boundary value problem (10, 12, 13) is described in detail in (Denisenko, 1998).



## 6 The Results of the Calculations

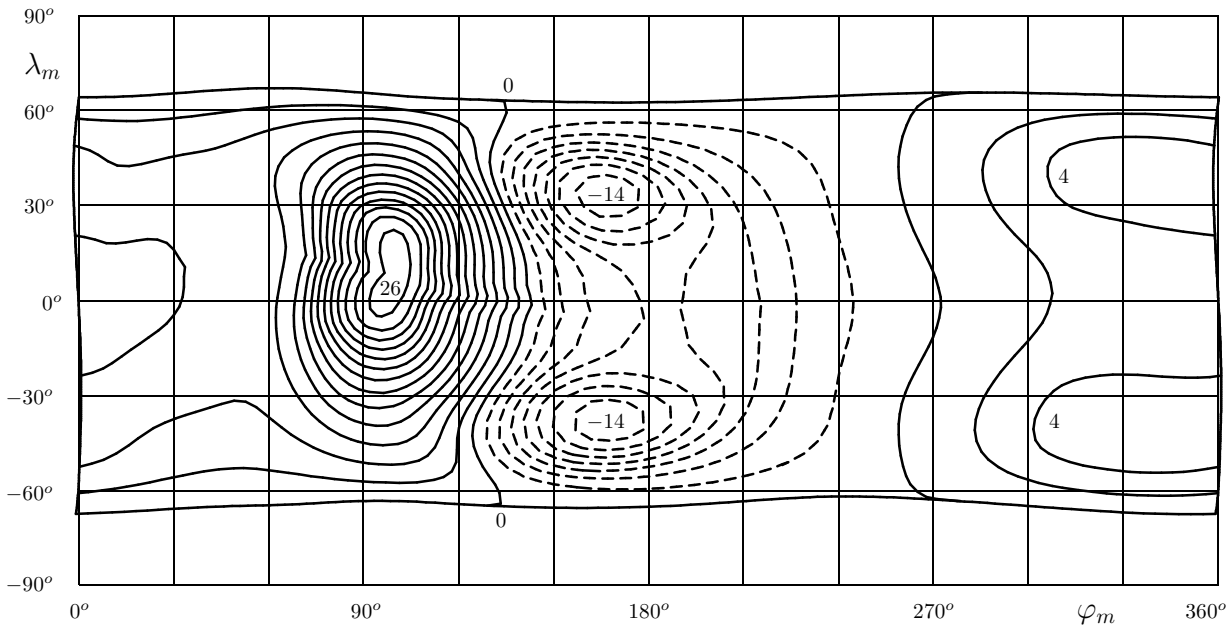


Рис. 5: Distribution of the electric potential at 120 km height in the ionosphere. Equipotentials are plotted with contour interval 2 V. Dashed lines correspond to negative values of potential. Maximum potential difference is about 42 V. Map is calculated under typical conditions for July under high solar activity at the considered point in time, 19:00 UT.

In the well known model (Hays, Roble, 1979) the ionospheric integral conductances were principally simplified as  $\Sigma_H \equiv 0$  and  $\Sigma_P \equiv 0.05 \text{ S}$ . The maximum potential difference within the ionosphere was 1575 V.

Due to the smaller height of the atmospheric column between the ground and the ionosphere above the Himalayas the column conductance is about 5 times larger. So the fair-weather current density has a maximum there and the minimum of the ionospheric electric potential is found just there.

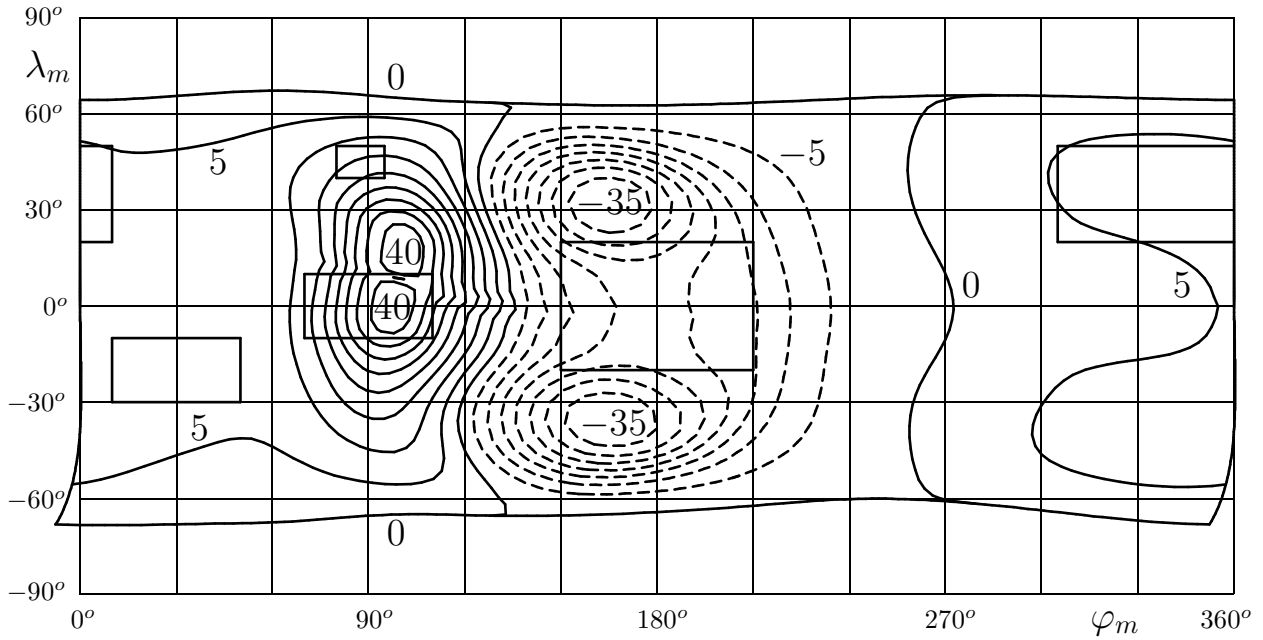


Рис. 6: Distribution of the electric potential at 120 km height in the ionosphere under low solar activity. Contour interval 5 V, maximum potential difference is about 86 V. The rectangles show the thunderstorm regions.

In our model the potential has identical values at the ionospheric conjugate points.

The model potentials in the ionosphere would be different from those presented in Fig. 3 at other times and under different solar activity conditions. Anyway the potential difference between ionospheric regions above thunderstorm areas and above fair-weather areas is always less than 200 V (Denisenko, et al., 2019).

The key parameters in our model: voltage between the ground and the ionosphere  $V_0 = 250$  kV, fair weather electric field near ground  $E_0 = 130$  V/m with corresponding current density  $j_0 = 2$  pA/m<sup>2</sup>, the total current flowing upwards from thundery areas to the ionosphere is  $I_{ext} = 1.4$  kA.

These values are considered to be typical for the GEC, but in view of the linearity of the model they could be multiplied by any common constant.

## 7 Conclusions

The obtained electric field in the ionosphere is an order of magnitude less than that in the model (Hays, Roble, 1979). The main reason for the different orders of magnitudes is a better approach for the simulation of the ionospheric conductivity in our model. That is our principal improvement to the model (Hays, Roble, 1979).

The research is supported by the Russian Foundation for Basic Research (project 18-05-00195).

## Bibliography

### Список литературы

- [1] Denisenko, V.V.: Multigrid method for a global Hall conductor in the Earth's ionosphere. Virtual Proceedings of the 10-th Anniversary International GAMM - Workshop on Multigrid Methods. (1998) <http://www.mgnet.org/mgnet-parm98.html>
- [2] Denisenko, V.V., Biernat, H.K., Mezentsev, A.V., Shaidurov, V.A., Zamay, S.S.: Modification of conductivity due to acceleration of the ionospheric medium. *Ann. Geophys.* 26, 2111-2130 (2008) doi:10.5194/angeo-26-2111-2008
- [3] Denisenko, V.V., Rycroft, M.J., Harrison, R.G.: Mathematical Simulation of the Ionospheric Electric Field as a Part of the Global Electric Circuit. *Surv. Geophys.* 40(1), 1-35 (2019). doi:10.1007/s10712-018-9499-6
- [4] Denisenko, V.V., Rycroft, M.J., Harrison, R.G.: Correction to: Mathematical Simulation of the Ionospheric Electric Field as a Part of the Global Electric Circuit. *Surv. Geophys.* 40(1), 37 (2019) doi: 10.1007/s10712-018-9505-z

- [5] Denisenko, V.V, Yakubailik, O.E.: The contribution of topography to the resistance of the global atmospheric conductor. *Solar-Terr. Ph.* 1(1), 104-108 (2015) doi:10.12737/6044 (in Russian)
- [6] Hays, P.B., Roble, R.G.: A quasi-static model of global atmospheric electricity. 1. The lower atmosphere. *J. Geophys. Res.* 84(A7), 3291-3305 (1979) doi:10.1029/JA084iA07p03291
- [7] Rycroft, M.J., Odzimek, A.: Effects of lightning and sprites on the ionospheric potential, and threshold effects on sprite initiation, obtained using an analog model of the global atmospheric electric circuit. *J. Geophys. Res.* 115:A00E37 (2010) doi:10.1029/2009JA014758